



## CHAPTER IV RESULTS AND DISCUSSION

### 4.1 Effect of Blend Composition on Drug Release

Drug releases from the drug-loaded chitosan/silk fibroin blend films containing chitosan contents of 100, 80, 60, 50 and 40% were studied at 37°C and pH 5.5 using modified Franz diffusion cells. However, drug release from the blend films with chitosan content less than 40% are not reported because the films were very brittle and difficult to handle without cracking. The results of drug release study are shown in Table 1. For all model drugs, the maximum drug releases were found for the blend film with 80% chitosan content. The amounts of theophylline, salicylic acid, diclofenac sodium and amoxicillin trihydrate released from the blend films with 80% chitosan content were 77.44%, 92.14%, 73.09% and 32.00%, respectively. Compared to pure chitosan films, the amounts of model drug released from the blend films with 80% chitosan content were higher than that released from pure chitosan film (Figure 1). It is known that the drug release from hydrogels is mainly controlled by swelling-controlled release mechanism (Peppas *et al.*, 1983). According to this, the degrees of swelling of chitosan and the blend films after releasing of drugs were investigated and the results are shown in Table 1. It was found that the maximum degrees of swelling of the drug-loaded films were obtained for the blend film with 80% chitosan content. This result is in good agreement with the study of Chen *et al.* (1997b). Chen *et al.* (1997b) studied on swelling behavior of glutaraldehyde-crosslinked chitosan and silk fibroin blend films and reported that the maximum degree of swelling was observed for the blend film with 80% chitosan content. For chitosan/silk fibroin blend film, hydrogen bonding between amino group of chitosan and amide group of silk fibroin can be formed at pH higher than pKa of amino groups of chitosan (pKa = 6.3-6.5). However, at pH less than the pKa, the protonation of amino group of chitosan occur and hydrogen bonding disappear, resulting in swelling state of the films. The dissociation of the hydrogen bonding between amino group of chitosan and the amide group of silk fibroin was shown in Figure 4.2 (Chen *et al.*, 1997b).

**Table 4.1** Drug release and degree of swelling of chitosan and the blend films of chitosan and silk fibroin

Model drug	Weight ratio of chitosan to silk fibroin	Drug release <sup>(a)</sup> (%)	Degree of swelling <sup>(a)</sup> (%)
Theophylline	100 : 0	66.26	708.82
	80 : 20	77.44	958.69
	60 : 40	58.37	389.45
	50 : 50	48.77	358.78
	40 : 60	40.04	313.41
Salicylic acid	100 : 0	87.31	951.23
	80 : 20	92.14	1056.87
	60 : 40	68.51	488.70
	50 : 50	65.20	441.29
	40 : 60	49.74	404.89
Diclofenac sodium	100 : 0	63.25	554.82
	80 : 20	73.09	663.04
	60 : 40	50.74	553.25
	50 : 50	27.00	502.68
	40 : 60	18.58	493.30
Amoxicillin	100 : 0	28.83	698.95
	80 : 20	32.00	940.48
	60 : 40	21.57	448.60
	50 : 50	18.83	398.95
	40 : 60	14.09	352.89

(a) The values at equilibrium state

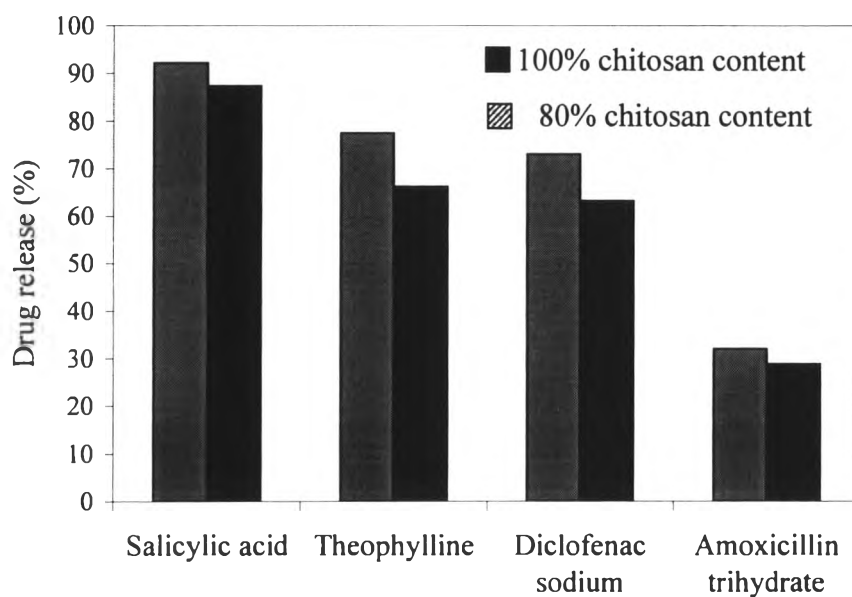


**Figure 4.1** Comparison of percentages of drug released from chitosan and the blend film with 80% chitosan content. (■) 100% chitosan content and (▨) 80% chitosan content.

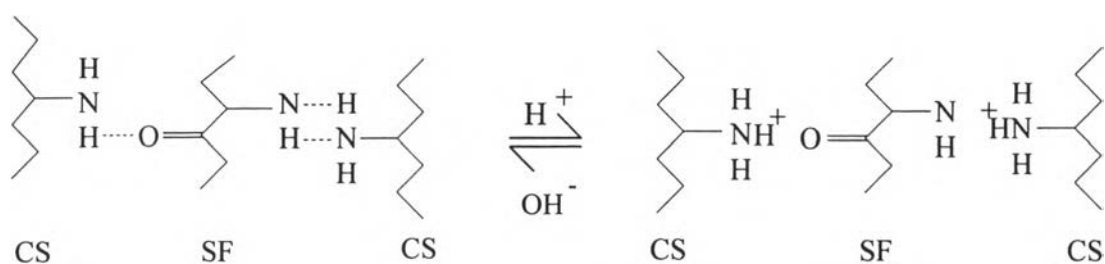


**Figure 4.2** Formation of hydrogen bond between chitosan (CS) and silk fibroin (SF) in the semi-interpenetrating network and the dissociation of chitosan and silk fibroin by breaking down the hydrogen bond in the acidic medium, Chen *et al.* (1997b).

Furthermore, it was found that as chitosan content in the blend films decreased from 80% to 40%, the degrees of swelling of the blend films as well as the releasing amounts of drug decreased. Since drug release property correlated to swelling behavior of the blend films and swelling ability of the blend films depended on the blend composition, it might be said that drug release from the blend films was influenced by the blend composition of the films. In addition to swelling-controlled release mechanism, drug release can be occurred by erosion process. According to this, the weight losses of the films after releasing of drug were also determined (data not shown). Since significant weight losses of the films could be observed, the release of drugs from the films might be occurred by erosion process as well.

#### 4.2 Effect of Drug Nature on Drug Release

Since all model drugs had the maximum drug releases for the blend film with 80% chitosan content, Figure 4.1 shows only the percentages of drug released from the blend film with this blend composition compared to those released from pure chitosan film. It was found that the order of drug from the highest release to the lowest release was as follows: salicylic acid > theophylline > diclofenac sodium > amoxicillin trihydrate. The same trends were obtained for the other blend compositions. The main factors that can affect the penetration of drug from a polymer matrix are molecular weight of drug, drug-polymer interaction and solubility of drug in the blend solution. When consider the molecular weights of model drugs that are 138, 180, 318 and 387 for salicylic acid, theophylline, diclofenac sodium and amoxicillin trihydrate, respectively, it can be seen that the order of drug above arranged from the model drugs with the lowest molecular weight to that with the highest molecular weight. It might be explained that the drug with lower molecular weight could penetrate from the network of the films easier than the drug with higher molecular weight.

Furthermore, the interaction between polymer matrix and drug also affect the drug release property of the films. The structures of model drugs are shown in Figure 4.3-4.6. For salicylic acid (Figure 4.3), there is carboxylic group in its molecule. Puttipatkhachorn *et al.* (2001) studied on drug-polymer interaction of

chitosan and salicylic acid. It has been reported that carboxylic group of salicylic acid could interact with amino group of chitosan by the formation of salicylate anion, as shown in Figure 4.7. Therefore, there might be some interaction between salicylic acid and chitosan in the blend films. For theophylline (Figure 4.4), there is no functional group that can react with either chitosan or silk fibroin in the blend films. In addition, Puttipipatkachorn *et al.* (2001) reported that there is no drug-polymer interaction between theophylline and chitosan. In this study, the interactions between chitosan and the model drugs were determined by FTIR technique and the results are shown in Figure 4.8-4.11. The FTIR spectrum of chitosan (Figure 4.8(a)) shows the symmetric carboxylate anion stretching at around  $1411\text{ cm}^{-1}$ , indicating that chitosan in the film was in the form of chitosonium acetate (Yao *et al.*, 1994). The characteristic peaks of NH group in chitosan appear at around  $1561\text{ cm}^{-1}$  (amino group of chitosan and amide II of chitin) and  $1257\text{ cm}^{-1}$  (amide III of chitin) (Figure 4.8(a)). Moreover, the characteristic peaks assigned to saccharide structure appear at around  $898\text{ cm}^{-1}$  and  $1153\text{ cm}^{-1}$  (Chen *et al.*, 1997a). For the silk fibroin film (Figure 4.8(b)), the absorption band at around  $1650\text{ cm}^{-1}$  (amide I) and  $1542\text{ cm}^{-1}$  (amide II) which are attributed to the random coil conformation were observed (Chen *et al.*, 1997a and Yoshimizu *et al.*, 1990). In case of salicylic acid (Figure 4.9(e)), the carbonyl stretching peak was observed at around  $1656\text{ cm}^{-1}$  (Moffat, 1986). For salicylic acid-loaded blend film, a new peak at around  $1628\text{ cm}^{-1}$  assigned to an asymmetric  $\text{NH}_3^+$  bending was observed (Figure 4.9(d)) (Silverstein *et al.*, 1991). A new peak was also observed at around  $1384\text{ cm}^{-1}$ , which was assigned to the symmetric carboxylate anion stretching of salicylate anion (Figure 4.9(d)). It might be indicated that salicylic acid could interact with chitosan at the position of amino group to form salicylate salt. This results were correlated to the results of Puttipipatkachorn *et al.* (2001) who studied the drug-polymer interaction of salicylic acid and theophylline in chitosan films by FTIR and solid state  $^{13}\text{C}$  NMR spectroscopy. In case of theophylline (Figure 4.8(e)), the absorption bands at around  $1720\text{ cm}^{-1}$  (C=O stretching),  $1676\text{ cm}^{-1}$ ,  $1567\text{ cm}^{-1}$  (C=C stretching),  $1485\text{ cm}^{-1}$  (C=N stretching),  $1314\text{ cm}^{-1}$  and  $1242\text{ cm}^{-1}$  (C-N, C-O vibration) were observed. For theophylline-loaded blend film (Figure 4.8(d)), the FTIR spectrum of theophylline-

loaded blend film did not show any new peak or peak shift indicating that no drug-polymer interaction was observed in theophylline-loaded blend films.

In case of diclofenac sodium, although diclofenac sodium has carboxylic group in its structure (Figure 4.5), it is difficult to interact with amino group of chitosan because of its bulky group. In this study, characteristic bands of diclofenac sodium (Figure 4.10(e)) were in 3350-3310  $\text{cm}^{-1}$  region (NH stretching vibration), 3100-3000  $\text{cm}^{-1}$  region (aromatic CH stretching vibration), 1600-1550  $\text{cm}^{-1}$  region (asymmetrical carboxyl stretching vibration) and around 1400  $\text{cm}^{-1}$  (symmetrical carboxyl stretching vibration) (Nasir *et al.*, 1996). The shift of peaks in the drug-loaded blend films was not observed in FTIR spectrum. It could be suggested that there was no interaction between polymer matrix and diclofenac sodium.

For amoxicillin trihydrate, similar to diclofenac sodium although the presence of carboxylic group in its molecule (Figure 4.6), it might not be able to interact with amino group of chitosan because its bulky group made it difficult to interact with chitosan. The FTIR spectrum of amoxicillin trihydrate is shown in Figure 4.11(e). Characteristic peaks were observed at around 1250  $\text{cm}^{-1}$  (phenol CO combination band), 1396  $\text{cm}^{-1}$  (dimethyl CH deformation and phenol OH combination band), 1482  $\text{cm}^{-1}$  (amide II, NH bending, CN stretching combination band and  $\text{NH}_3^+$  symmetric deformation), 1686  $\text{cm}^{-1}$  (amide I, CO stretch) and 1775  $\text{cm}^{-1}$  ( $\beta$ -lactam CO stretching) (Brittain, 1994). The FTIR peaks of amoxicillin trihydrate did not change when amoxicillin trihydrate was loaded into chitosan/silk fibroin blend film. Therefore, it might be suggested that there was no interaction between chitosan and amoxicillin trihydrate.

Therefore, among four model drugs, salicylic acid was the only one that possibly had interaction with chitosan in the blend films. The effect of this drug-polymer interaction on drug release could be observed in drug release profile of salicylic acid as shown in Figure 4.12(a). It was found that the release of salicylic acid had an initial lag time that the other model drugs did not have. It might be suggested that the initial lag time was spent for dissociation of the interaction between salicylic acid and chitosan before the release of drug occurred. In addition, the solubility of drug in the blend solution is another factor that can affect the drug release. The solubility in water of salicylic acid, theophylline, diclofenac sodium and

amoxicillin trihydrate are 2.17 mg/ml, 8.3 mg/ml, 21 mg/ml and 1-10 mg/ml, respectively (Brittain, 1994 and Florey, 1975). From our results, although the solubility of diclofenac was higher than that of salicylic acid, the releasing amounts of diclofenac were less than those of salicylic acid. It might be explained that drug release property resulted from a combination of various factors, e.g. molecular weight of drug, interaction between drug and polymer matrix and solubility of drug. However, in this study, molecular weights of model drugs seem to be a dominant factor that influenced drug release property of chitosan/silk fibroin blend films.

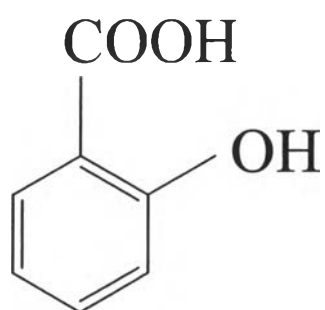


**Figure 4.3** Structure of salicylic acid.

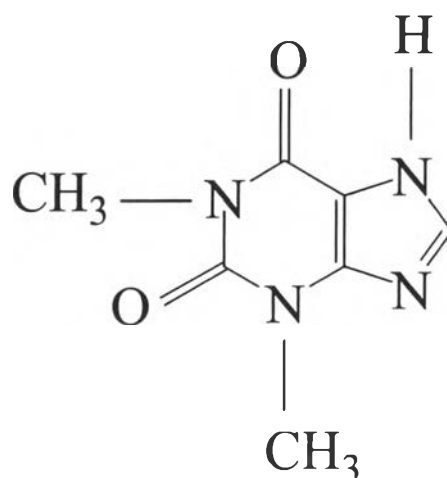


**Figure 4.4** Structure of theophylline.

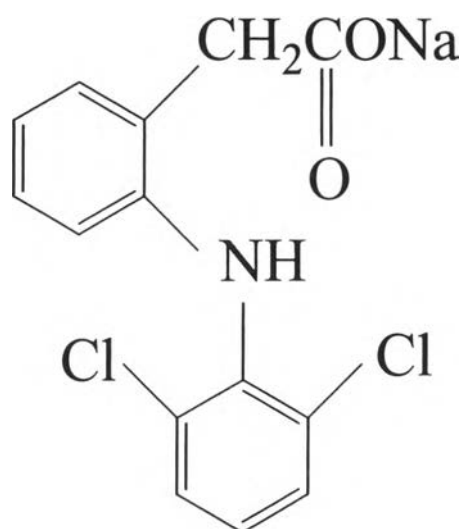


**Figure 4.5** Structure of diclofenac sodium.

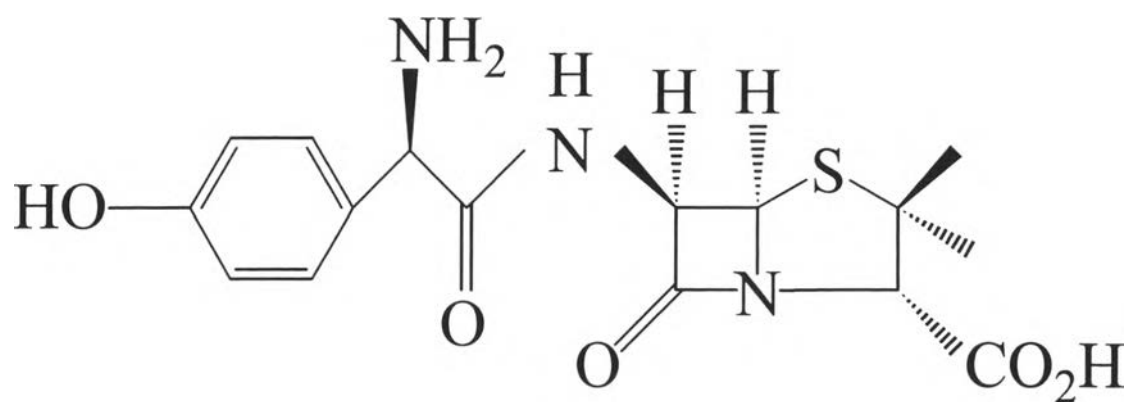


**Figure 4.6** Structure of amoxicillin trihydrate.



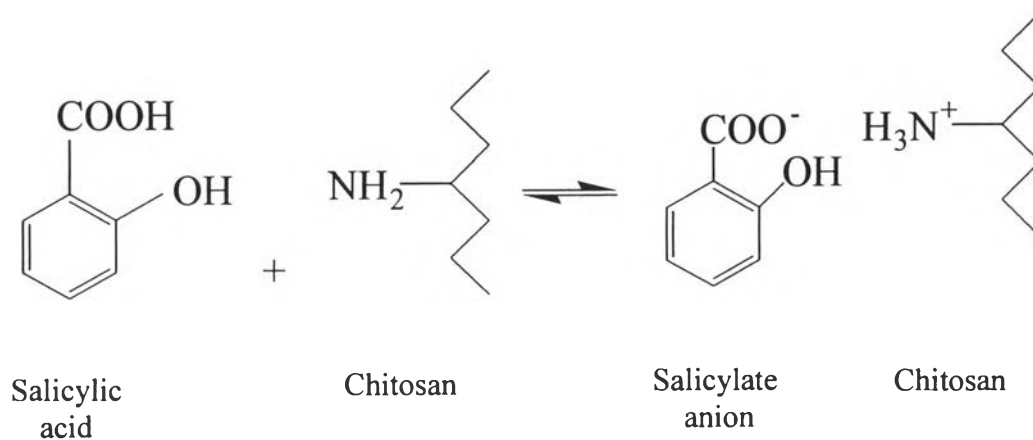


**Figure 4.7** Interaction between salicylic acid and chitosan.

**Table 4.2** FTIR characteristic absorption bands of chitosan

Frequencies ( $\text{cm}^{-1}$ )	Assignment and remarks
1411	Symmetric $\text{COO}^-$ stretch
1561	Amino group of chitosan and amide II of chitin
1257	Amide III of chitin
1153, 898	Saccharide structure

**Table 4.3** FTIR characteristic absorption bands of silk fibroin

Frequencies ( $\text{cm}^{-1}$ )	Assignment and remarks
1650	Amide I, $\text{C}=\text{O}$ stretching
1542	Amide II, $\text{N-H}$ bending and $\text{C-N}$ stretching

**Table 4.4** FTIR characteristic absorption bands of theophylline

Frequencies (cm <sup>-1</sup> )	Assignment and remarks
1720	C=O stretching
1676, 1567	C=C stretching
1485	C=N stretching
1446	C-H bending
1314, 1242	C-N, C-O vibration

**Table 4.5** FTIR characteristic absorption bands of salicylic acid

Frequencies (cm <sup>-1</sup> )	Assignment and remarks
1656	C=O stretching
1628	Asymmetric NH <sub>3</sub> <sup>+</sup>
1440	C=C stretching
1384	Asymmetric COO <sup>-</sup>
690,760	Aromatic C-H bending

**Table 4.6** FTIR characteristic absorption bands of diclofenac sodium

Frequencies (cm <sup>-1</sup> )	Assignment and remarks
3350-3310	N-H stretching
3100-3000	Aromatic C-H stretching vibration
1600-1550	Asymmetrical C=O stretching vibration
1400	Symmetrical C=O stretching vibration

**Table 4.7** FTIR characteristic absorption bands of amoxicillin trihydrate

Frequencies (cm <sup>-1</sup> )	Assignment and remarks
1775	β-lactam C=O stretching
1686	amide I, C=O stretching
1482	amide II, N-H bending and C-N stretching
1396	dimethyl C-H deformation and phenol -OH
1250	phenol C=O

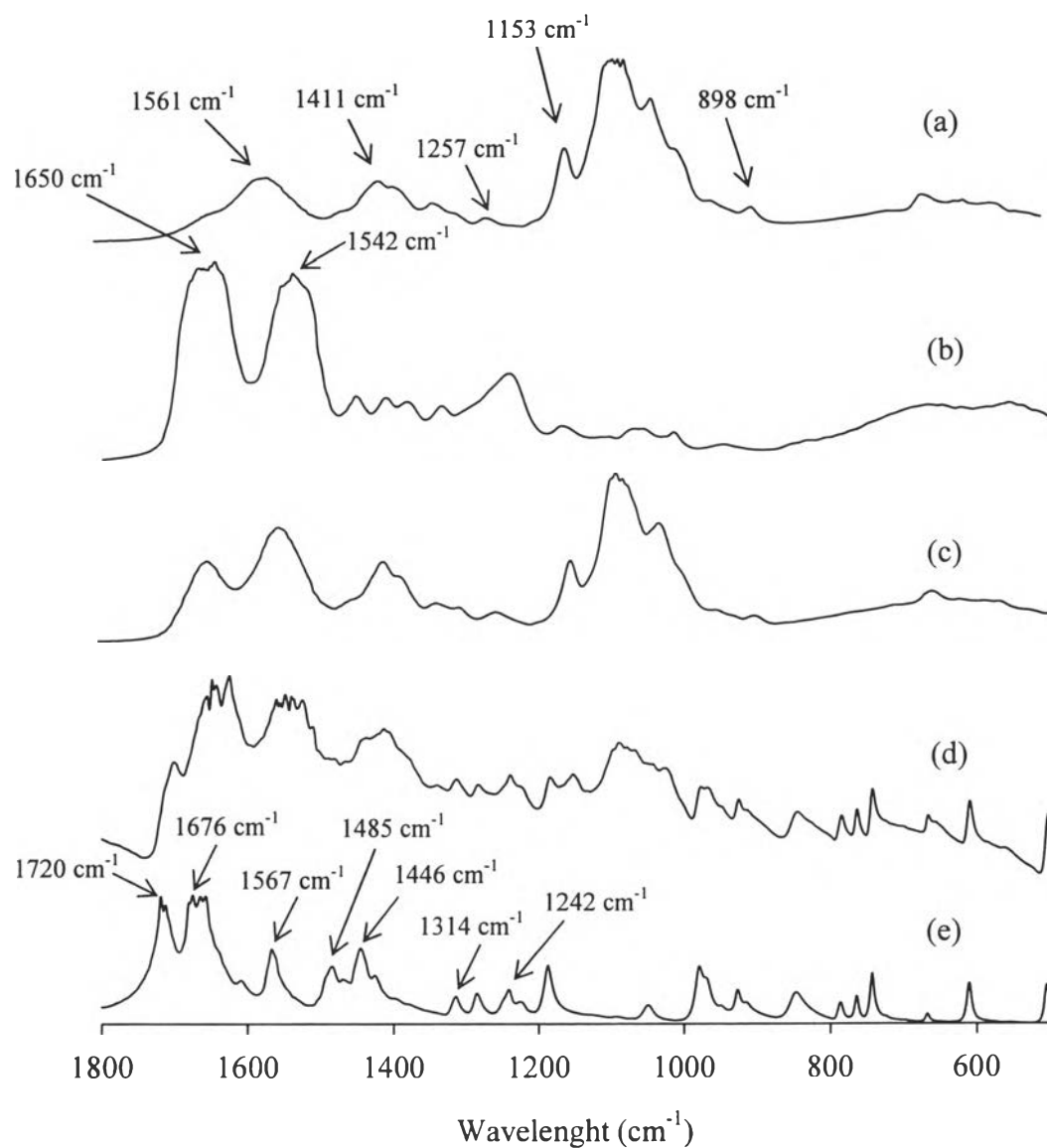


**Figure 4.8** FTIR spectra of (a) chitosan film, (b) silk fibroin film, (c) blend film with 80% chitosan content, (d) theophylline-loaded blend films with 80% chitosan content and (e) theophylline.

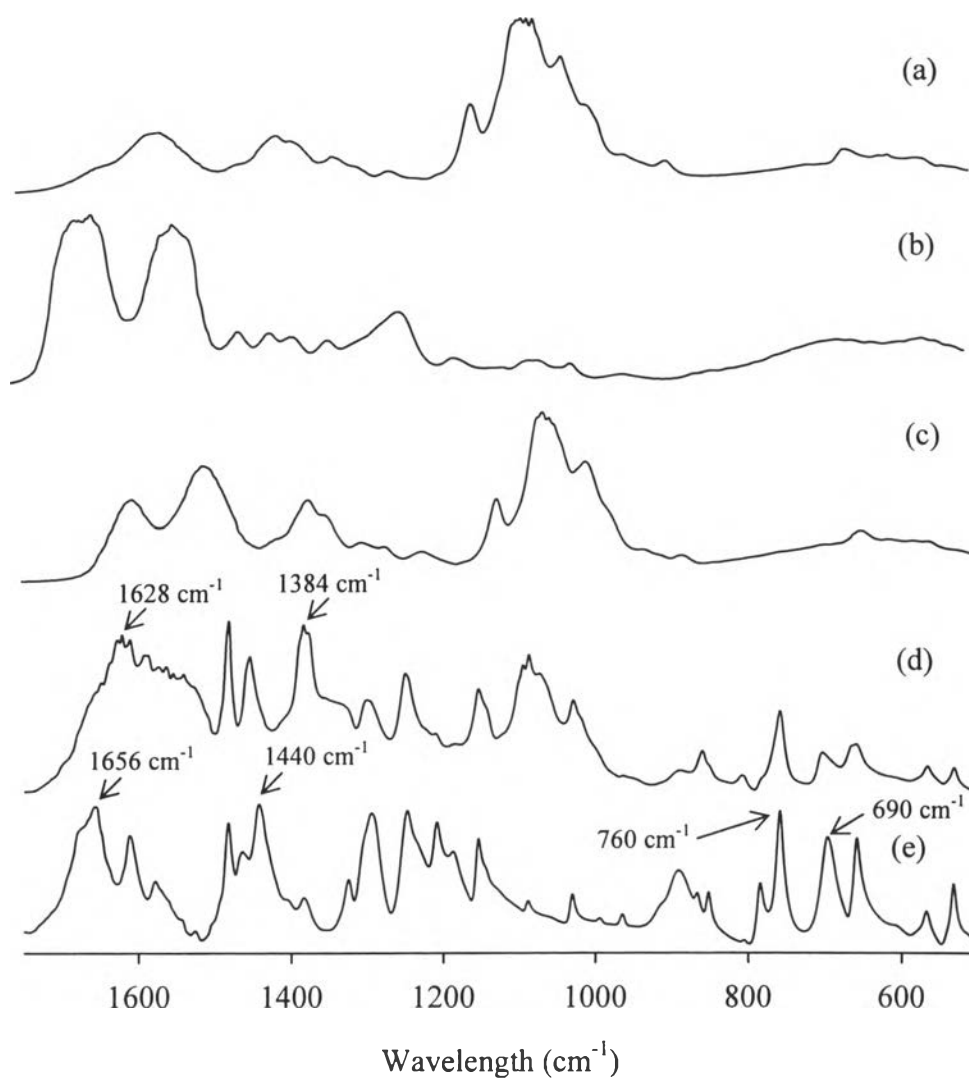


**Figure 4.9** FTIR spectra of (a) chitosan film, (b) silk fibroin film, (c) blend film with 80% chitosan content, (d) salicylic acid-loaded blend films with 80% chitosan content and (e) salicylic acid.

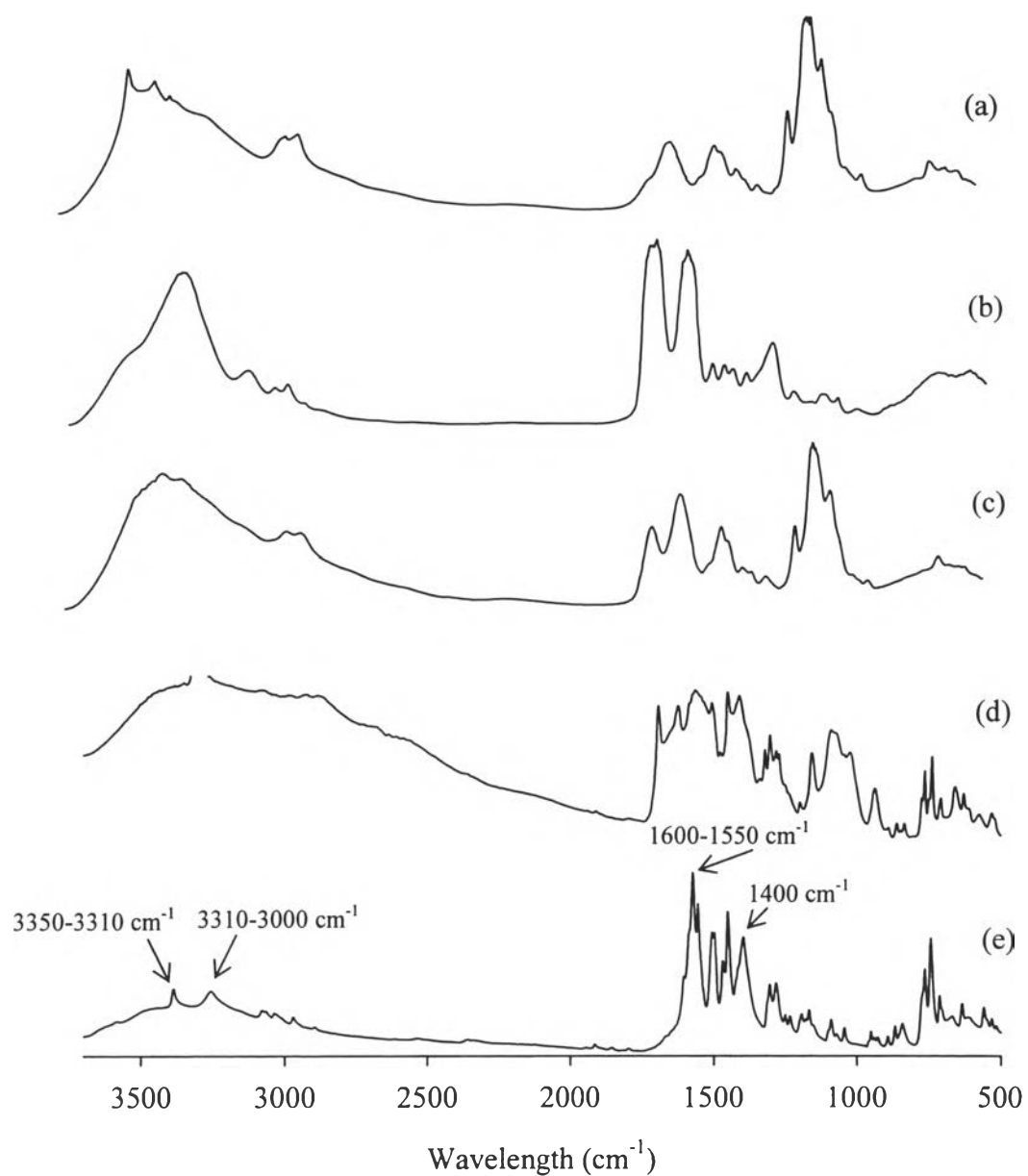


**Figure 4.10** FTIR spectra of (a) chitosan film, (b) silk fibroin film, (c) blend film with 80% chitosan content, (d) diclofenac sodium-loaded blend films with 80% chitosan content and (e) diclofenac sodium.

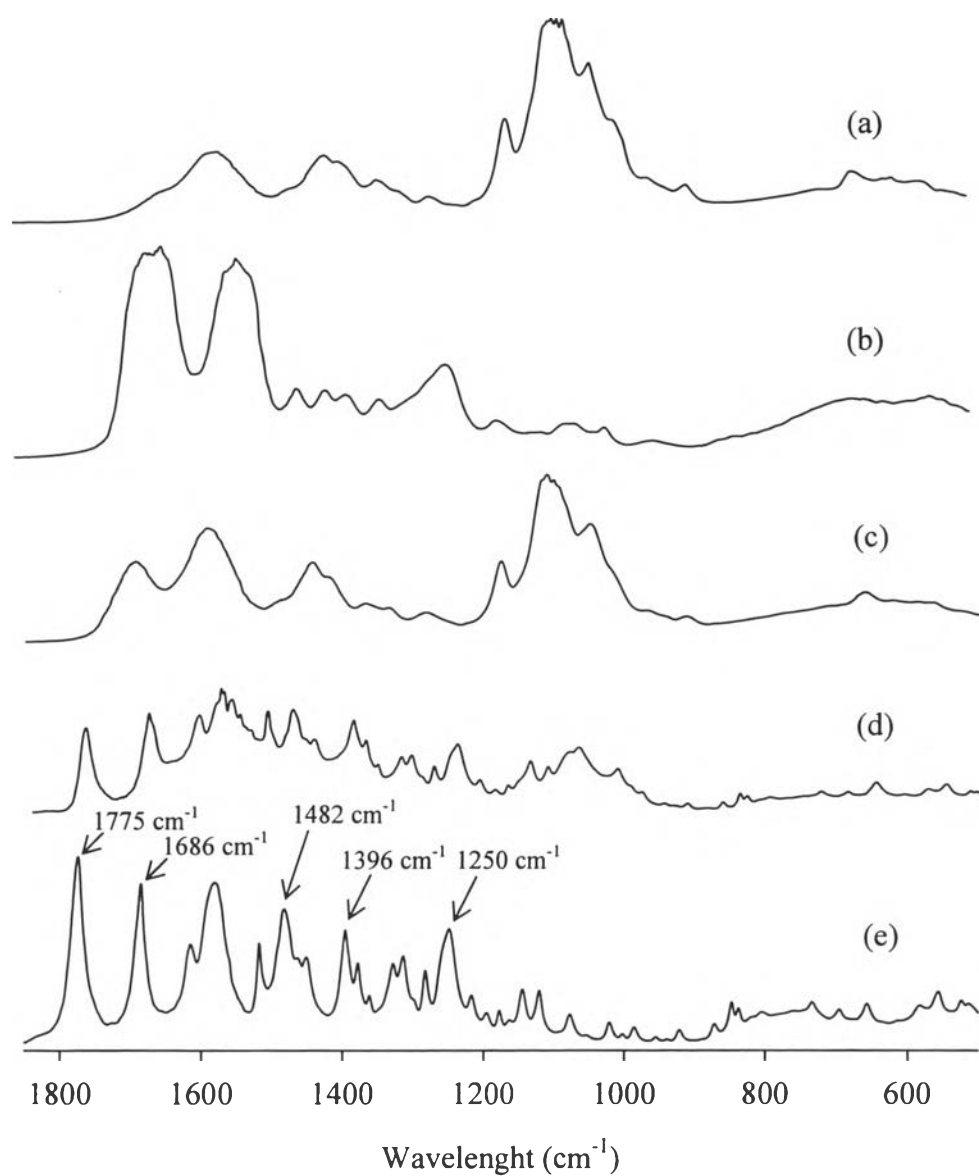


**Figure 4.11** FTIR spectra of (a) chitosan film, (b) silk fibroin film, (c) blend film with 80% chitosan content, (d) amoxicillin trihydrate-loaded blend films with 80% chitosan content and (e) amoxicillin trihydrate.

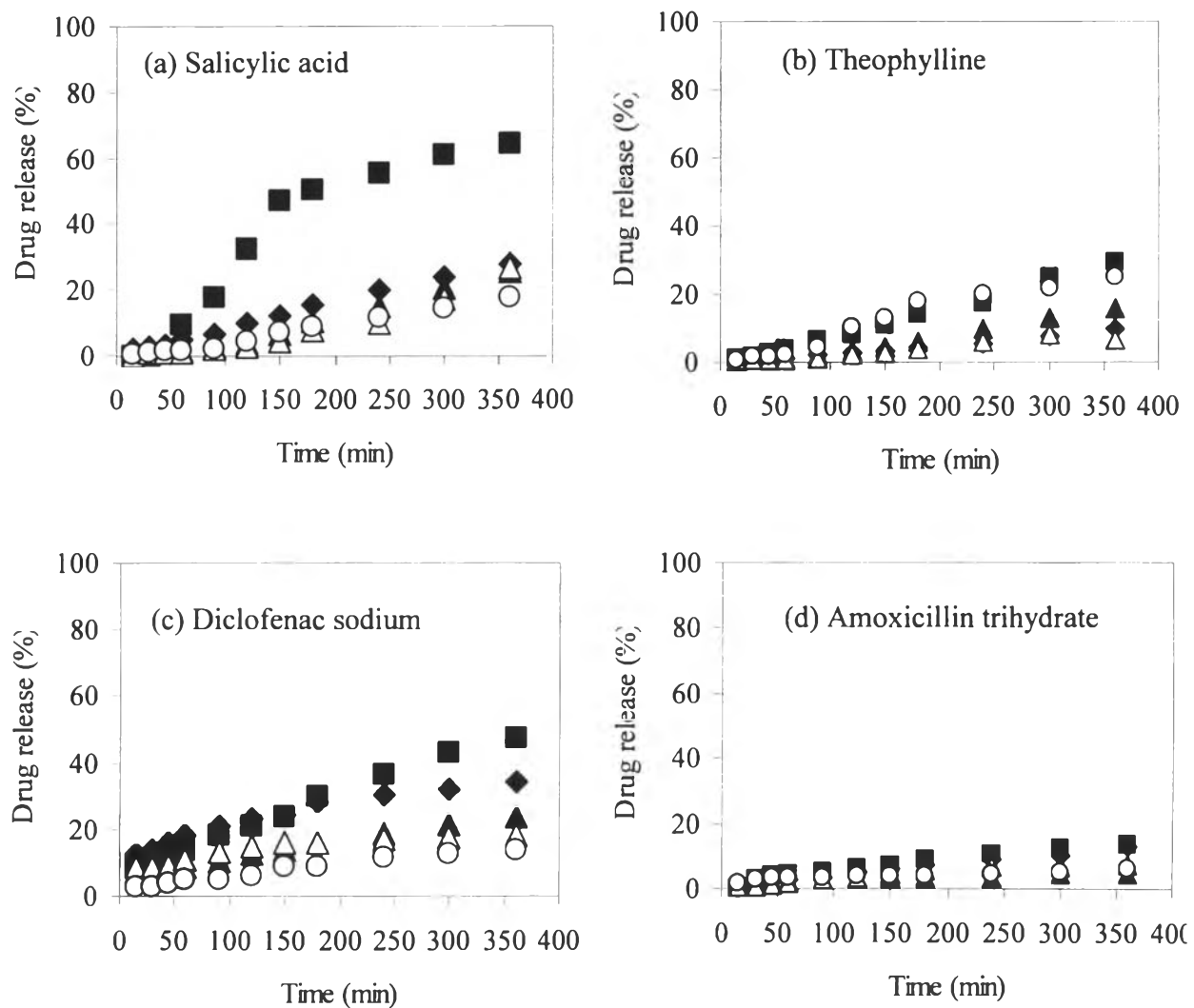


**Figure 4.12** Drug release profile for pure chitosan and the blend films. (◆) 100% chitosan content, (■) 80% chitosan content, (▲) 60% chitosan content, (△) 50% chitosan content and (○) 40% chitosan content.

### 4.3 Effect of Releasing Time on Drug Release

The release profiles of each model drug for chitosan and the blend films are illustrated in Figure 4.13-4.16. The releasing amounts of drug from the films increased as releasing time increased until reached the equilibrium. It is known that the release of drug from hydrogel is controlled by swelling-controlled mechanism. According to this, swelling behavior of chitosan and the blend films as a function of time were also investigated using the diffusion cell. The results on swelling behavior of chitosan and the blend films at 37°C and pH 5.5 are shown in Figure 4.17. The degree of swelling of chitosan and the blend films remarkably increased at the initial stage and finally reached the equilibrium. At the initial stage when the dry films contacted with the pig skin saturated with pH 5.5 at 37°C, the solution from the pig skin diffused into the films leading to swollen stage of hydrogel. At this stage, when the films became swollen, the drug inside the films would penetrate out of the films. The diffusion of water into the films and the diffusion of drugs from the films occurred until the films reached the equilibrium state.

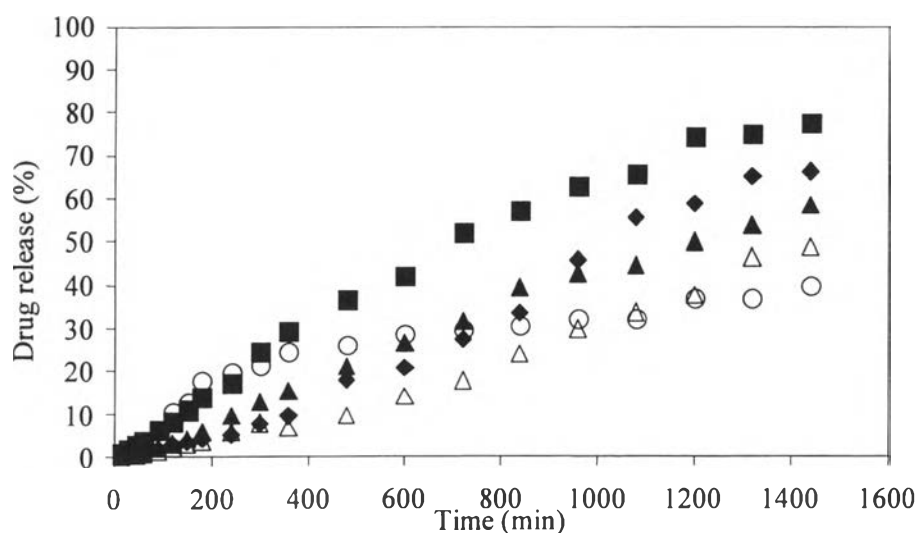


**Figure 4.13** Effect of releasing time on releasing of theophylline. (◆) 100% chitosan content, (■) 80% chitosan content, (▲) 60% chitosan content, (△) 50% chitosan content and (○) 40% chitosan content.



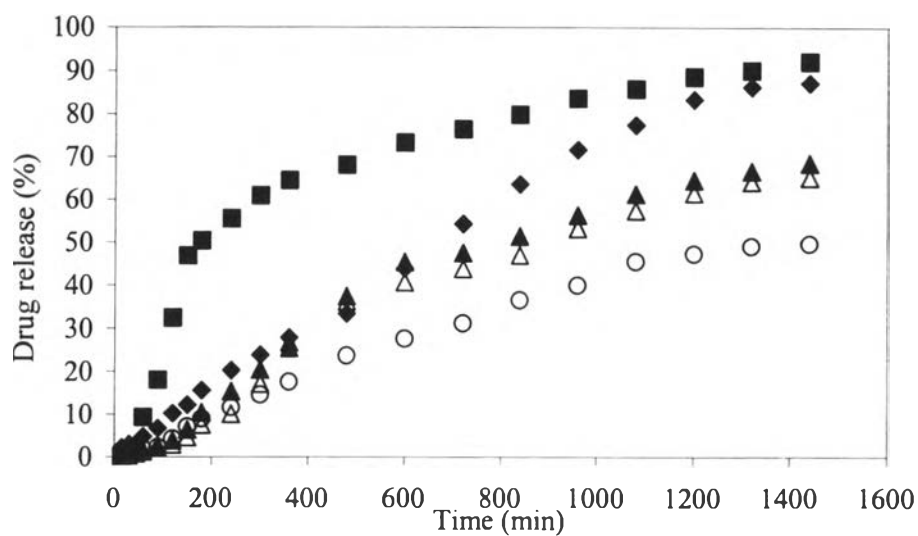


**Figure 4.14** Effect of releasing time on releasing of salicylic acid. (◆) 100% chitosan content, (■) 80% chitosan content, (▲) 60% chitosan content, (△) 50% chitosan content and (○) 40% chitosan content.

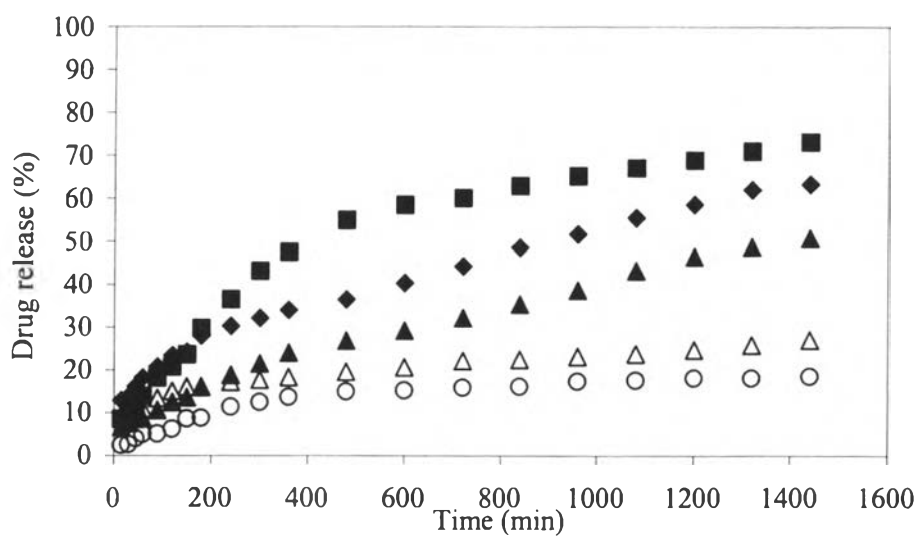


**Figure 4.15** Effect of releasing time on releasing of diclofenac sodium. (◆) 100% chitosan content, (■) 80% chitosan content, (▲) 60% chitosan content, (△) 50% chitosan content and (○) 40% chitosan content.

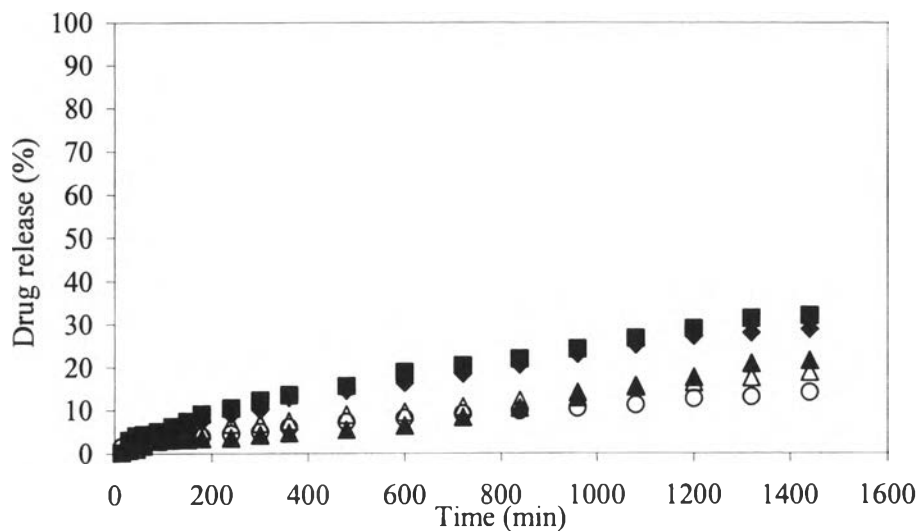


**Figure 4.16** Effect of releasing time on releasing of amoxicillin trihydrate. (◆) 100% chitosan content, (■) 80% chitosan content, (▲) 60% chitosan content, (△) 50% chitosan content and (○) 40% chitosan content.

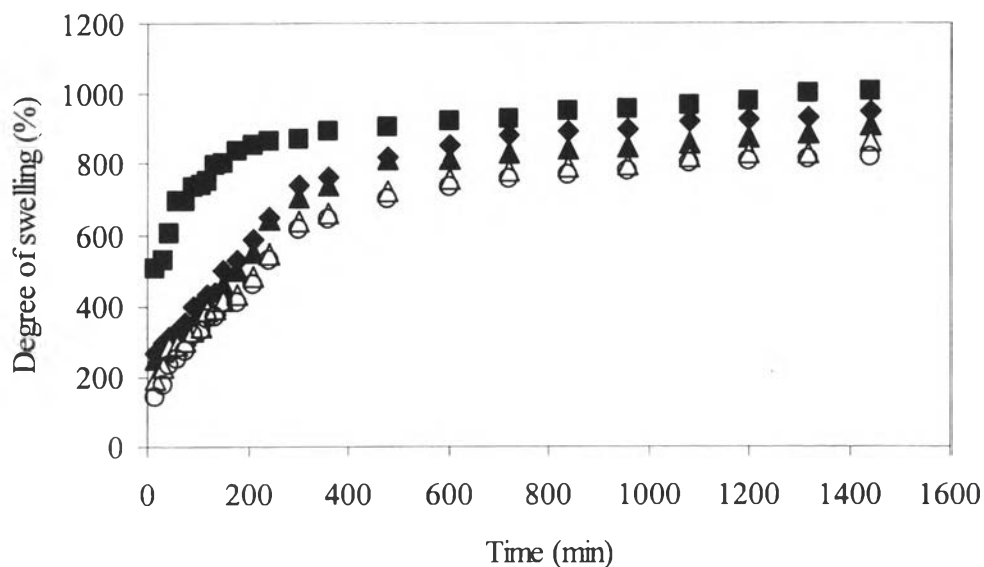


**Figure 4.17** Degree of swelling of chitosan/silk fibroin blend films as a function of time (◆) 100% chitosan content, (■) 80% chitosan content, (▲) 60% chitosan content, (△) 50% chitosan content and (○) 40% chitosan content.

#### 4.4 Effect of Thickness on Drug Release

Since the length of diffusion distance concerns the thickness of films, the effect of the film thickness on drug release was investigated and the results are shown in Figure 4.18. The experiment was done for the blend film with 80% chitosan content and the model drug used was theophylline. The three ranges of thickness studied were 20-30  $\mu\text{m}$ , 50-60  $\mu\text{m}$  and 100-120  $\mu\text{m}$ . It was found that the amount of theophylline released from the films with the thickness of 20-30  $\mu\text{m}$ , 50-60  $\mu\text{m}$  and 100-120  $\mu\text{m}$  were 77.44%, 14.92% and 10.41%, respectively. The more thickness of the film, the longer diffusion path. This resulted in the lower amounts of drug released. Therefore, the thin film is recommended to obtain high amount of released drug.

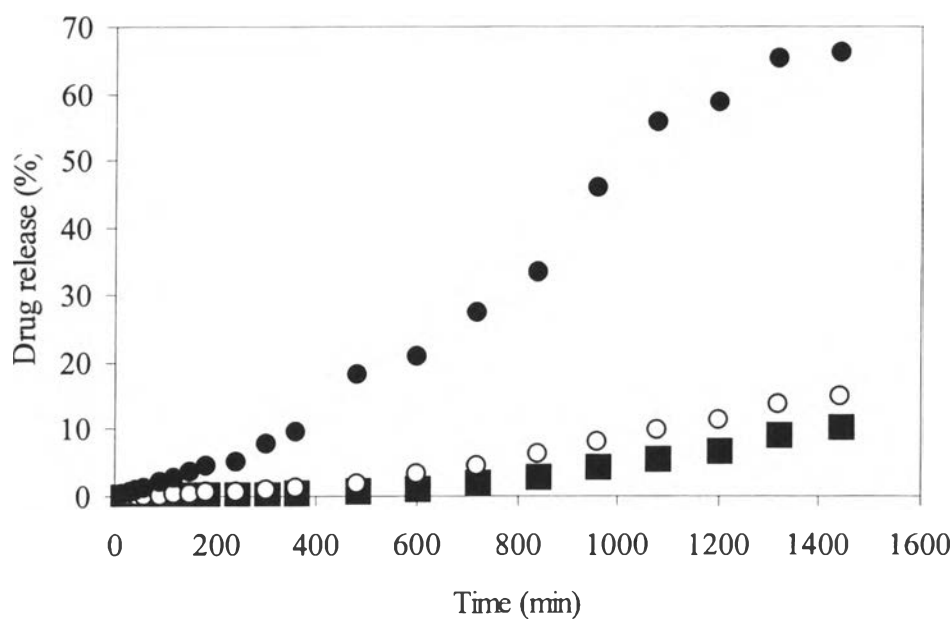


**Figure 4.18** Drug release profile for theophylline-loaded blend films with 80% chitosan content. The thickness of the films were (●) 20-30  $\mu\text{m}$ , (○) 50-60  $\mu\text{m}$  and (■) 100-120  $\mu\text{m}$ .

## 4.5 Kinetics

For kinetics of drug release, there are four models, i.e. zero order kinetic, Higuchi's model, first order kinetic and model for laminate structure. However, the last model concerns a film with multilayer that did not study in this work. In order to determine the kinetics of drug release, the most linearity which obtained from the correlation between  $M_t/M_\infty$  versus time (zero order kinetic) and  $M_t/M_\infty$  versus square root of time (Higuchi's model) were used, where  $M_t/M_\infty$  is the fraction of drug released up to time  $t$ . The correlation coefficient ( $R^2$ ) for each model was analyzed and compared to each other. The model that had correlation coefficient result closed to the value one was chosen to explain the behavior of those data. For the first order kinetic, the relationship between  $\log M_t/M_\infty$  and time was also plotted. However, it was found that the correlation coefficients of the first order kinetic were much less than the value one for all model drugs and all blend compositions. Therefore, the first order kinetic was not considered in this study.

In this study, it was found that all model drug release data were fitted to either zero order or Higuchi's model. Figure 4.19-4.26 shows normal plots (percent drug release versus time) that is for zero order kinetic and Higuchi's plots (percent drug release versus square root of time). The normal plots for zero order kinetic model show linear profile that increase with releasing time. Permeability of drug did not change as the drug concentration changed with time. It could be said that no matter how much drug left in the film, the drug release came out at constant rate with the increasing of releasing time. Therefore, zero order kinetic model informed that the blend films which drug pass through were rate-controlling membrane. Higuchi's plots show linear profile in term of drug release and square root of releasing time. It has been indicated that the drug release from the blend films in Higuchi's model was diffusion-controlled release in which the release of drug depends on the concentration of drug remaining in the films. The analytical results of model drug release kinetics were showed in Table 4.8.

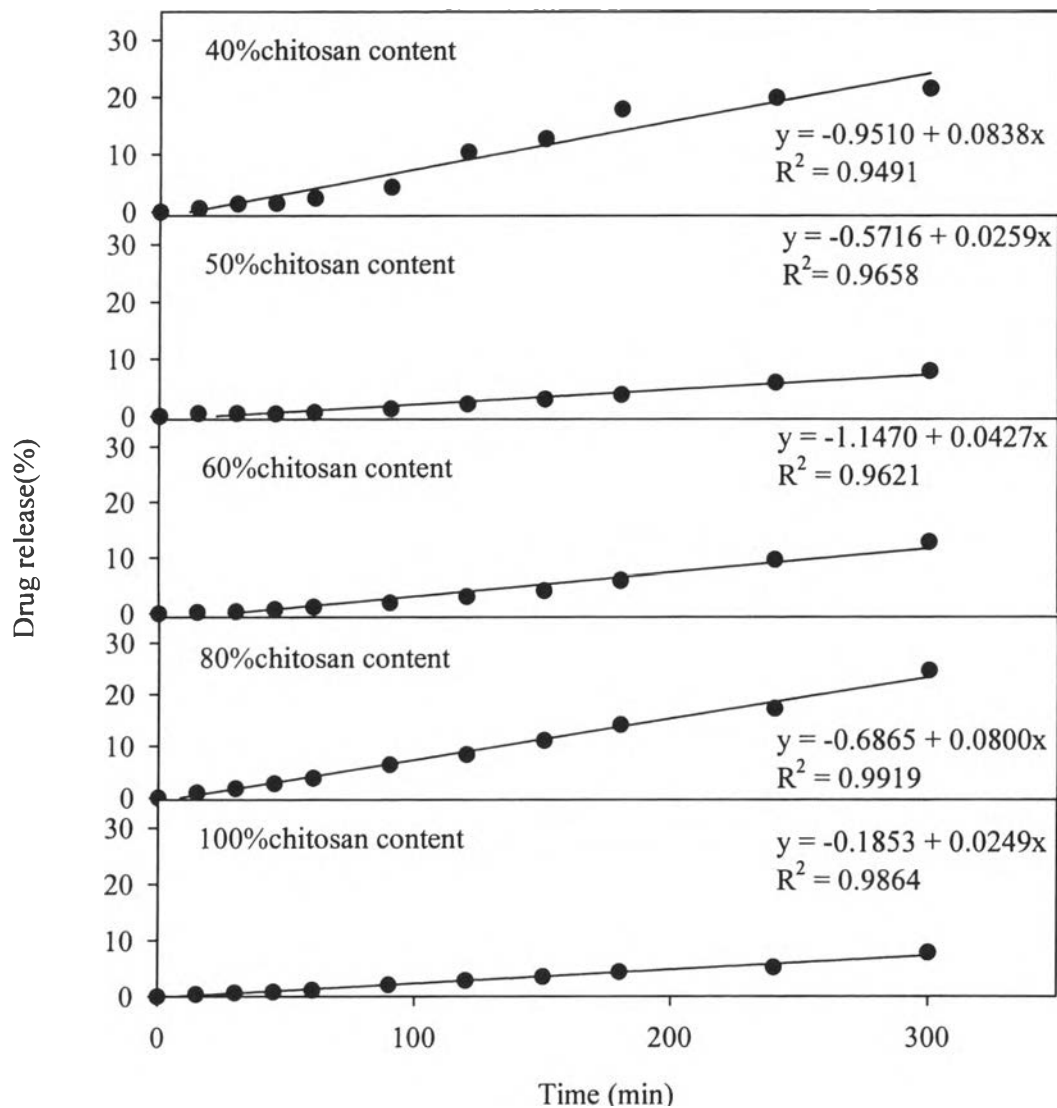


**Figure 4.19** Normal plot of releasing of theophylline from chitosan/silk fibroin blend films with different blend composition at 37°C and pH 5.5.

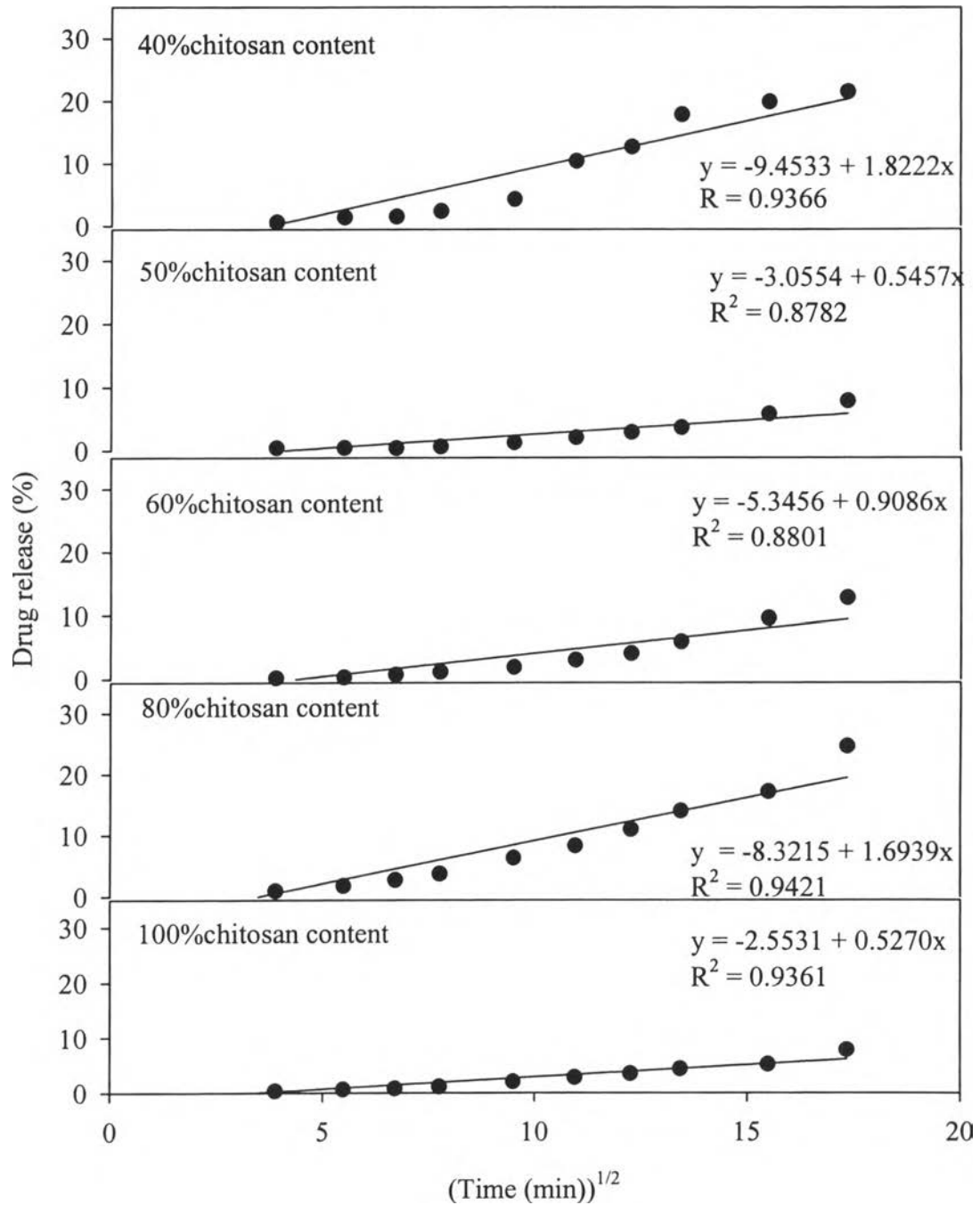


**Figure 4.20** Higuchi plot of releasing of theophylline from chitosan/silk fibroin blend films with different blend composition at 37°C and pH 5.5.

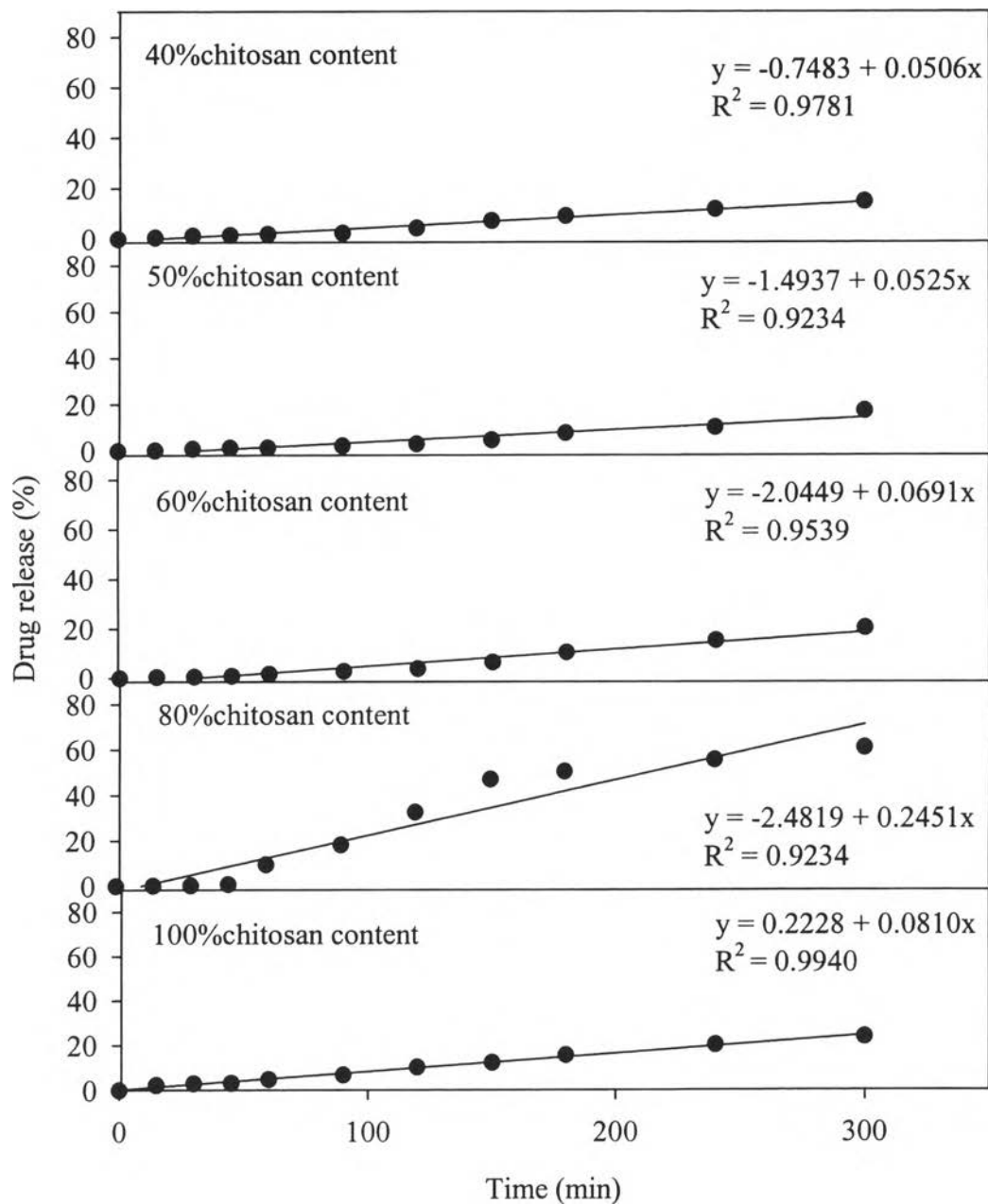


**Figure 4.21** Normal plot of releasing of salicylic acid from chitosan/silk fibroin blend films with different blend composition at 37°C and pH 5.5.

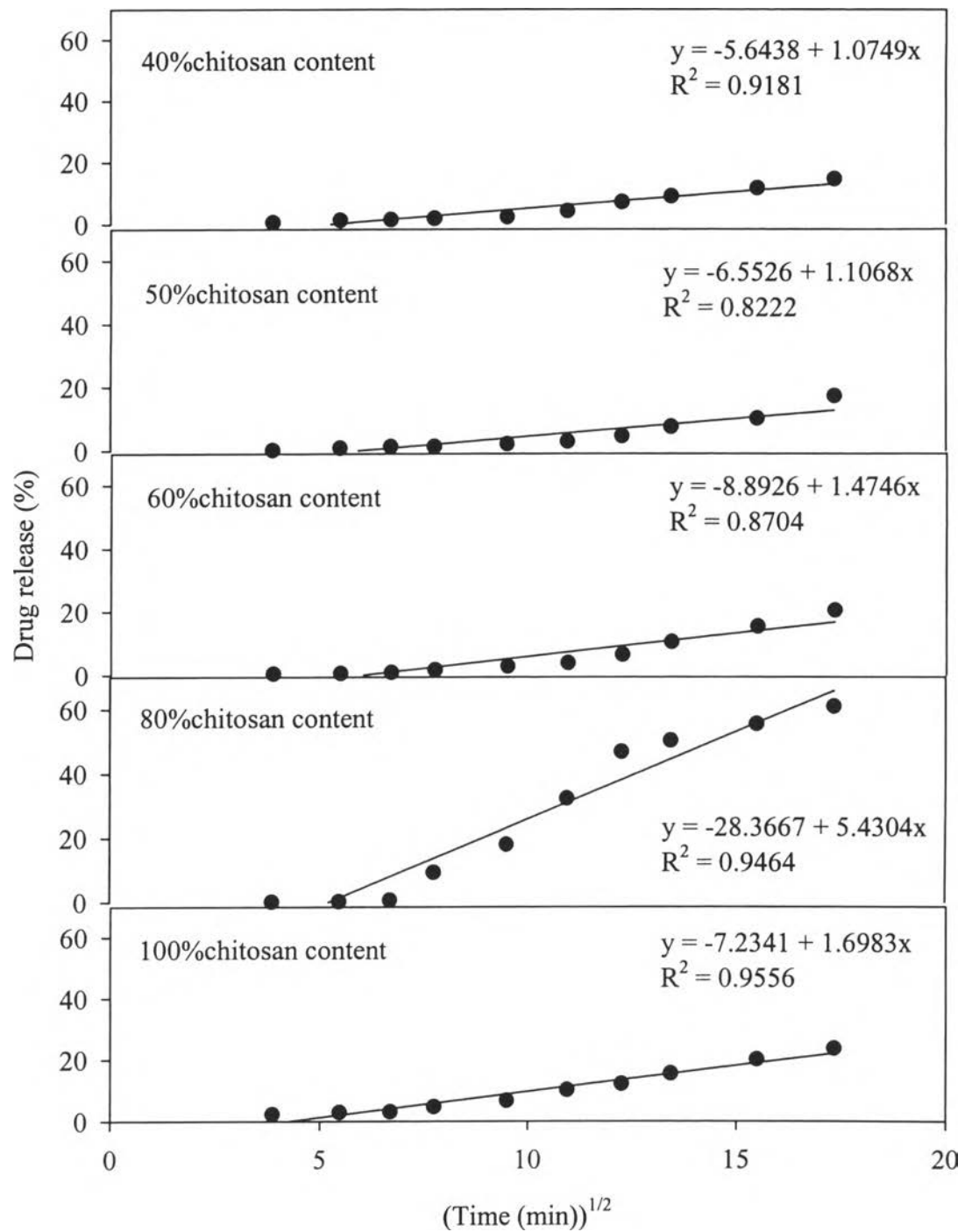


**Figure 4.22** Higuchi plot of releasing of salicylic acid from chitosan/silk fibroin blend films with different blend composition at 37°C and pH 5.5.



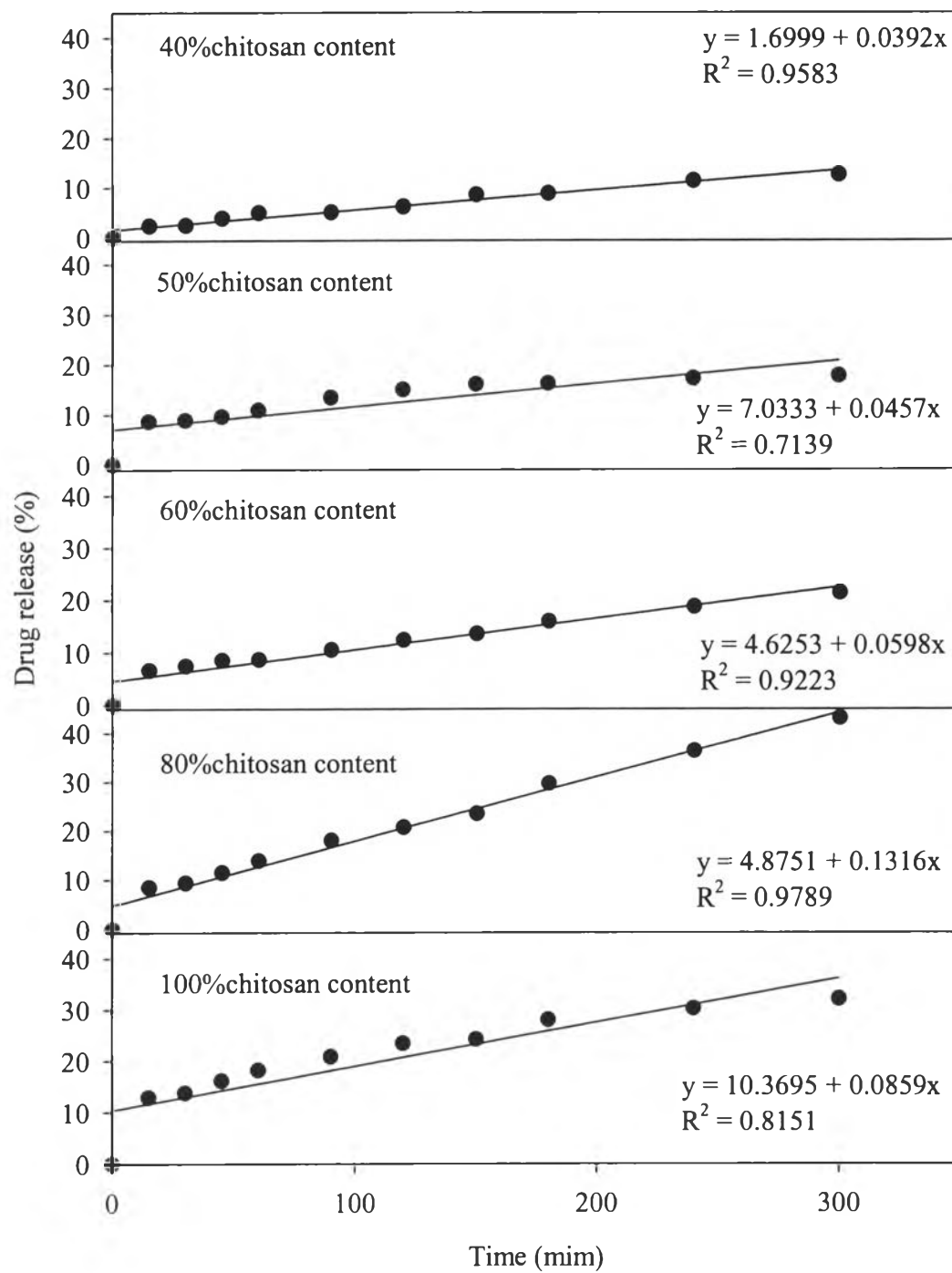


**Figure 4.23** Normal plot of releasing of diclofenac sodium from chitosan/silk fibroin blend films with different blend composition at 37°C and pH 5.5.

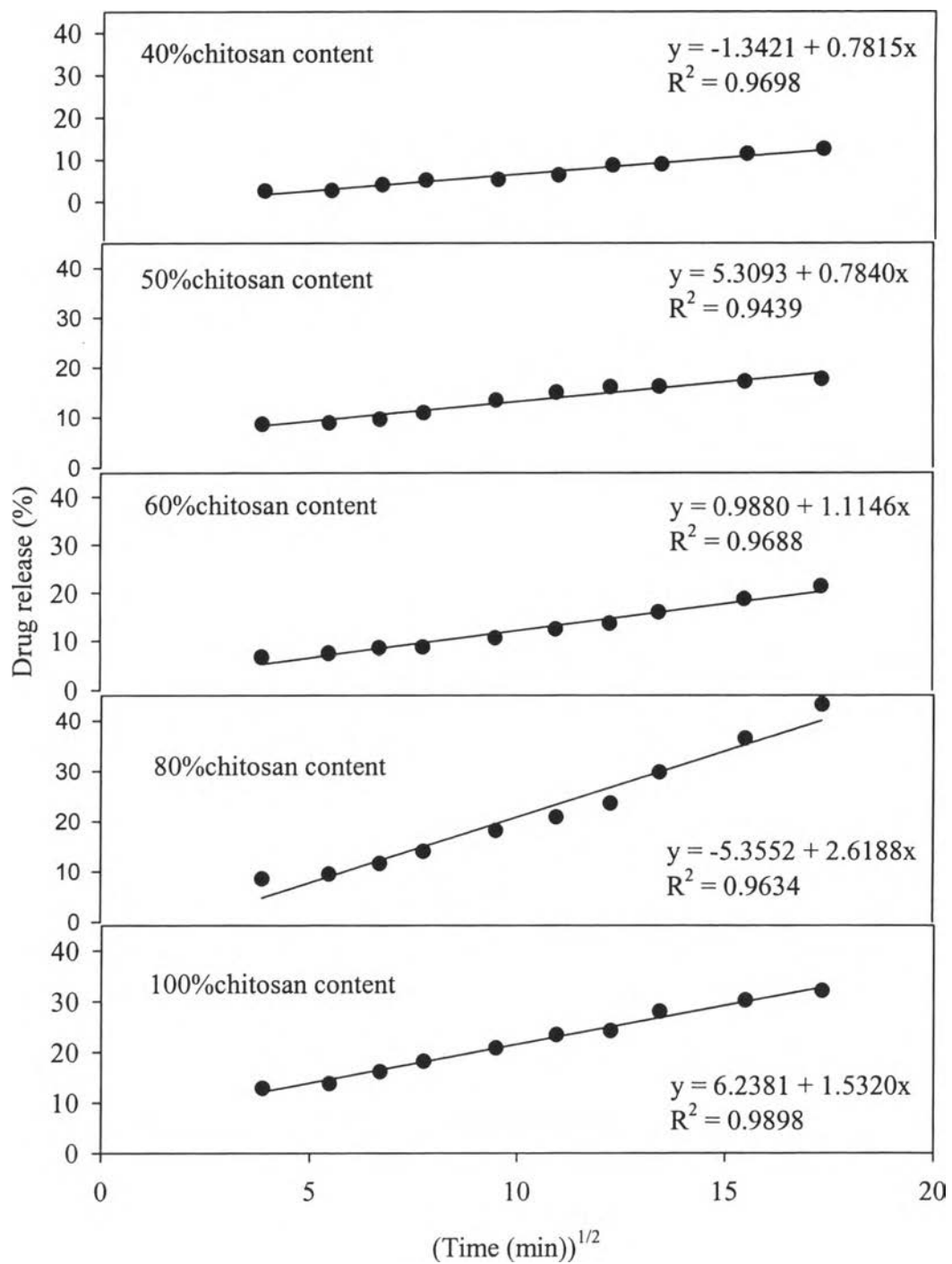


**Figure 4.24** Higuchi plot of releasing of diclofenac sodium from chitosan/silk fibroin blend films with different blend composition at 37°C and pH 5.5.

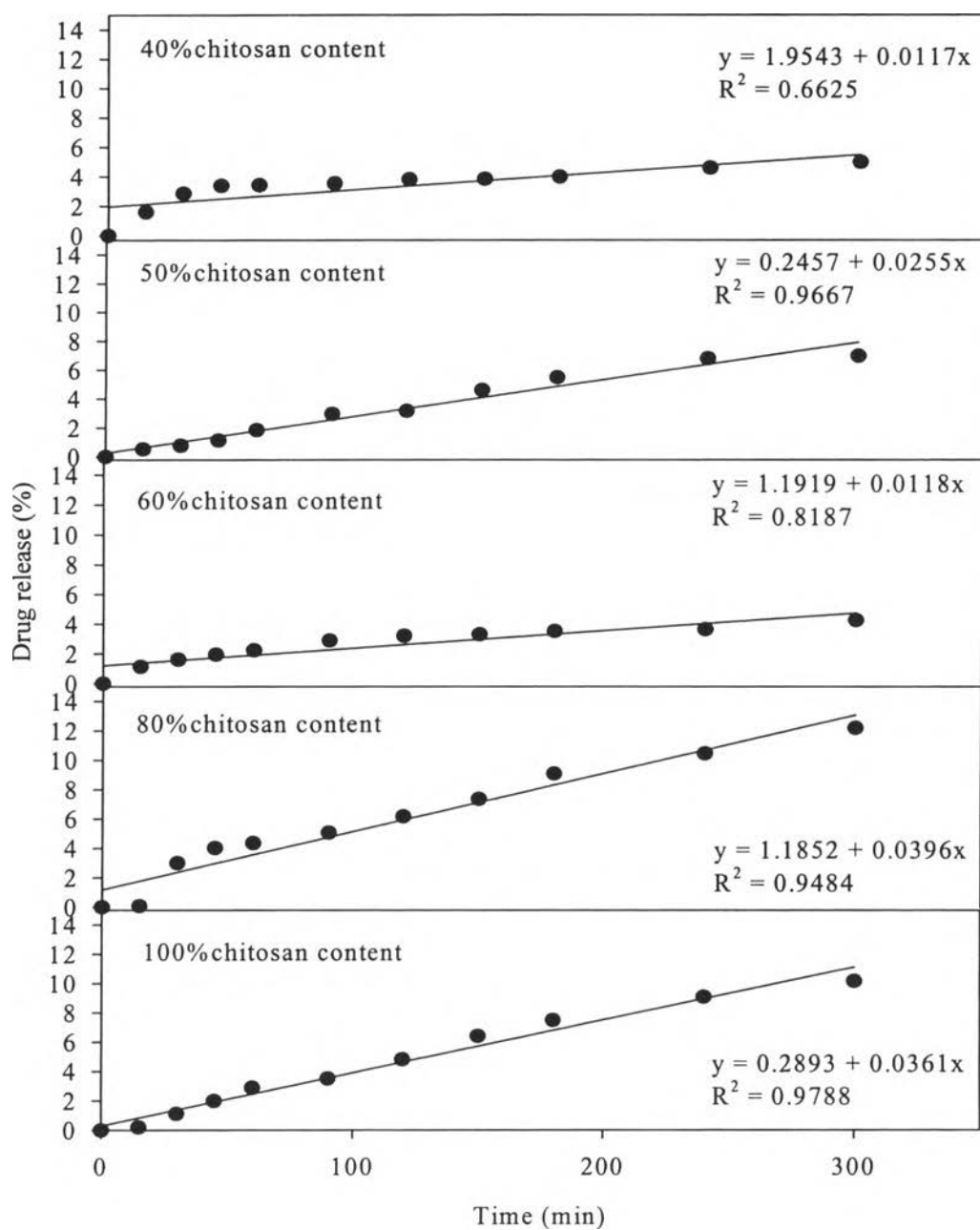


**Figure 4.25** Normal plot of releasing of amoxicillin trihydrate from chitosan/silk fibroin blend films with different blend composition at 37°C and pH 5.5.

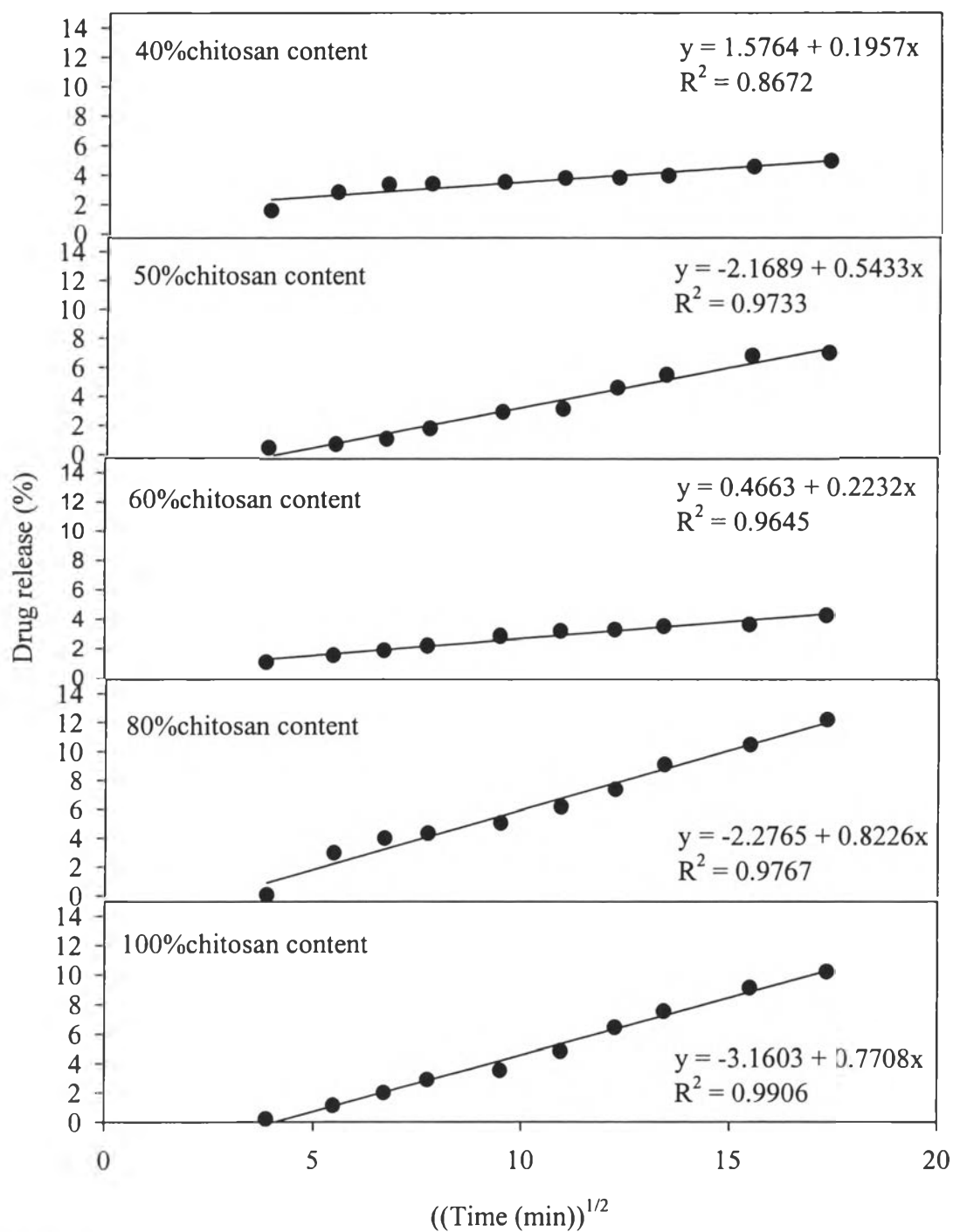


**Figure 4.26** Higuchi plot of releasing of amoxicillin trihydrate from chitosan/silk fibroin blend films with different blend composition at 37°C and pH 5.5.

**Table 4.8** The analysis of model-drug release kinetics

Model drugs	Weight ratio of chitosan to silk fibroin	Correlation coefficient		Kinetic pattern
		$M_t/M_\infty^{(a)}$ vs. t	$M_t/M_\infty^{(a)}$ vs. $(t)^{1/2}$	
Theophylline	100:0	0.9864	0.9361	Zero order
	80:20	0.9919	0.9421	Zero order
	60:40	0.9621	0.8801	Zero order
	50:50	0.9658	0.8782	Zero order
	40:60	0.9491	0.9366	Zero order
Salicylic acid	100:0	0.9940	0.9556	Zero order
	80:20	0.9234	0.9464	Higuchi model
	60:40	0.9539	0.8704	Zero order
	50:50	0.9234	0.8222	Zero order
	40:60	0.9781	0.9181	Zero order
Diclofenac sodium	100:0	0.8151	0.9898	Higuchi model
	80:20	0.9789	0.9634	Zero order
	60:40	0.9223	0.9688	Higuchi model
	50:50	0.7139	0.9439	Higuchi model
	40:60	0.9583	0.9698	Higuchi model
Amoxicillin	100:0	0.9788	0.9906	Higuchi model
	80:20	0.9484	0.9767	Higuchi model
	60:40	0.8187	0.9645	Higuchi model
	50:50	0.9667	0.9733	Higuchi model
	40:60	0.6625	0.8672	Higuchi model

<sup>(a)</sup> $M_t/M_\infty$  is the fraction of drug release up to time t.